NMR of *Chromatium vinosum* Ferredoxin: Evidence for Structural Inequivalence and Impeded Electron Transfer between the Two [4Fe-4S] Clusters

J. Gaspard Huber,‡ Jacques Gaillard,*,‡ and Jean-Marc Moulis§

CEA, Département de Recherche Fondamentale sur la Matière Condensée, SESAM-SCPM, and Laboratoire des Métalloprotéines, Département de Biologie Moléculaire et Structurale, Centre d'Etudes Nucléaires de Grenoble, 17 Rue des Martyrs, 38054 Grenoble Cédex 9, France

Received August 8, 1994; Revised Manuscript Received October 24, 1994⊗

ABSTRACT: The 2[4Fe-4S] ferredoxin from *Chromatium vinosum* has been investigated by ^{1}H and ^{13}C nuclear magnetic resonance. ^{1}H NMR sequence-specific assignments have been obtained for a large majority of the residues. They indicate that the protein folds along a pattern similar to that previously evidenced for shorter 2[4Fe-4S] ferredoxins. However, *C. vinosum* ferredoxin differs from other ferredoxins by the occurrence of a turn in an eight amino acid region separating two successive cysteines, Cys-40 and Cys-49, liganding one cluster. Also, the unique C-terminal end of *C. vinosum* ferredoxin contains a 10 amino acid α-helix which interacts with one side of the above turn. The only cysteine of the sequence not involved in the ligation of the [4Fe-4S] clusters is Cys-57. Specific NMR experiments helped characterizing the signals arising from the ligands of these clusters: most of them display properties reminiscent of those of homologous ferredoxins, except for the signals associated with Cys-40. Despite the general similarity between *C. vinosum* ferredoxin and other 2[4Fe-4S] ferredoxins, the electron paramagnetic resonance and NMR spectra of the former reduced protein are significantly different from those previously observed for $S = {}^1/_2$ [4Fe-4S]$^+$ clusters. In addition, the intramolecular electron transfer rate in *C. vinosum* is far slower than in other similar cases. This is the first report of impeded electron exchange between two [4Fe-4S] clusters expected to be less than 12 Å apart.

The ferredoxins (Fd)[1] containing two [4Fe-4S] clusters are iron−sulfur proteins occurring in numerous organisms (Cammack, 1992). These short proteins of as few as 55 amino acids are supposed to have arisen from the duplication of an ancestral gene encoding half of the primary structure (Eck & Dayhoff, 1966). As a result, most 2[4Fe-4S] ferredoxins display a molecular 2-fold axis relating one of its clusters and the nearby residues to the other cluster and corresponding residues (Adman et al., 1973, 1976; Backes et al., 1991; Duée et al., 1994). These proteins cycle between the [4Fe-4S]$^+$ and [4Fe-4S]$^{2+}$ levels and function as low-potential electron carriers in a variety of reactions (Cammack, 1992).

Among such ferredoxins, some isolated from photosynthetic purple bacteria form a group characterized by the presence of a 6−8 amino acid insertion between the second and third cysteines of the CxxCxxC-binding motif associated with the second [4Fe-4S] cluster (Otaka & Ooi, 1987). Less characteristically, these proteins have nine cysteines as potential ligands to the centers, although sequence alignments suggest that the cysteine closest to the C-terminus is not involved in the binding of the clusters (Matsubara & Saeki, 1992). The function(s) of these proteins has not been unambiguously established, but some clues about the involvement of the product of *fdxN* in the nitrogen fixation system of *Rhodobacter capsulatus* have been obtained (Saeki et al., 1991; Schmehl et al., 1993). In the so far unique case of Cv Fd, a 22 amino acid extension at the C-terminus sets the protein apart from the other 2[4Fe-4S] ferredoxins (Hase et al., 1977; Figure 1). The measured reduction potential of the latter protein is somewhat lower than the average −400 mV vs NHE usually found for 2[4Fe-4S] ferredoxins: values lower than −480 mV (Stombaugh et al., 1976) and of −460 mV (Smith & Feinberg, 1990) have been reported.

Since relatively little information is available for ferredoxins from photosynthetic bacteria, ^{1}H and ^{13}C NMR studies of 2[4Fe-4S] Cv Fd are presented herein. The proteins containing [4Fe-4S] clusters have recently proved amenable to almost complete sequence-specific assignments through ^{1}H NMR, despite the strong perturbation introduced by the electronic spin of the clusters (Nettesheim et al., 1992; Gaillard et al., 1992; Bertini et al., 1994). These data provide some indication about the main structural elements of such proteins in solution. Moreover, the study of the hyperfine-shifted protons in a ferredoxin like that of Cv, which differs considerably from the more common clostridial-type, may help validate the recently established model for the paramagnetic shifts in [4Fe-4S] proteins (Busse et al., 1991; Mouesca et al., 1993; Bertini et al., 1994) and should be

* Address correspondence to this author at DRFMC/SESAM/SCPM CENG, 17 Rue des Martyrs, 38054 Grenoble Cedex 9, France. Telephone: (33) 76 88 35 98. Fax: (33) 76 88 50 90. E-mail: gaillard@drfmc.ceng.cea.fr.

‡ SESAM-SCPM.

§ Laboratoire des Métalloprotéines.

⊗ Abstract published in *Advance ACS Abstracts,* December 1, 1994.

[1] Abbreviations: COSY, 2D correlation spectroscopy; DIPSI, decoupling in the presence of scalar interactions; EXSY, exchange spectroscopy; MCOSY, magnitude COSY; HMQC, heteronuclear multiple-quantum coherence; NOE, nuclear Overhauser effect; NOESY, 2D nuclear Overhauser enhancement spectroscopy; TOCSY, total correlation spectroscopy; WEFT, water eliminated Fourier transform; Cau, *Clostridium aciduric*i; Cp, *Clostridium pasteurianum*; Cv, *Chromatium vinosum*; Pas, *Peptostreptococcus asaccharolyticus*; Fd, ferredoxin; NHE, normal hydrogen electrode; DSS, 2,2-dimethyl-2-silapentane-5-sulfonate;

0006-2960/95/0434-194$09.00/0

instrumental in revealing the detailed redox properties of these ferredoxins.

MATERIALS AND METHODS

(a) Growth of Bacteria and Protein Purification. Cv (DSM 180) was grown and crude extracts were prepared as previously described (Gaillard et al., 1992). Ferredoxin was separated from most other redox proteins on a DEAE-cellulose column equilibrated in 0.2 M Tris-HCl, pH 7.4. The ferredoxin fractions were eluted with the same buffer containing 0.4 M NaCl and further purified by ammonium sulfate precipitation between 40 and 75% saturation at 4 °C. The 75% pellet was suspended in a minimal volume of 0.2 M Tris-HCl, pH 7.4 and dialyzed overnight against 10 mM Tris-HCl, pH 7.4. The desalted solution was concentrated on an Amicon YM5 membrane and filtrated through a Sephadex G-50 column equilibrated with 20 mM Tris-HCl, pH 7.4, and 50 mM NaCl. The last eluted gold-brown fraction was loaded on a hydroxylapatite column equilibrated in the same buffer, washed with 5 mM, and eluted with 50 mM sodium phosphate, pH 7.5. A last purification step was carried out on a PL-SAX HPLC column developed with a NaCl gradient in 20 mM sodium phosphate buffer at pH 7.5. The resulting material was at least as pure as formely reported (Bachofen & Arnon, 1966) according to its UV−visible spectrum.

For NMR experiments, ferredoxin samples, at a final concentration of ca. 1 mM, in 20 mM sodium phosphate buffer at pH 7.5 were brought to the desired pH in an Amicon cell fitted with a YM5 membrane. TOCSY and NOESY spectra were recorded in 15 mM potassium phosphate buffer at pH 6.0 containing 40 mM NaCl with 15% (v/v) D_2O for the lock. One of these samples was exchanged with 20 mM potassium phosphate at the uncorrected pH of 7.4 prepared in 99.95% D_2O (CEA-Oris, Gif-sur-Yvette, France).

Cv Fd was reduced by the addition of a 3-fold excess of sodium dithionite. To maintain a low ambiant potential, 20 μM methyl viologen and elemental Zn were also added to these samples.

(b) NMR Spectroscopy. 1D and 2D experiments were performed on a Varian Unity plus spectrometer operating at 500 MHz and using a reverse detection probe as described previously (Gaillard et al., 1993a). ^1H NMR chemical shifts were referenced relative to the water signal resonance, set at 4.72 ppm at 20 °C. ^{13}C NMR chemical shifts were referenced relative to external DSS in D_2O.

The water signal was suppressed by a low-power selective irradiation before the first pulse of each transient, and, for nontotally deuterated samples, a jump−return "reading" pulse (Plateau & Guéron, 1982) replaced the last pulse of the sequence. Spectra were recorded with a spectral width of 13 000 Hz (60 000 Hz for the reduced samples), restricted to 5700 Hz for the study of non-hyperfine-shifted signals.

1D NMR experiments in D_2O were recorded with 96 scans. T_1 values of the most shifted signals were measured at 293 K using the standard nonselective inversion−recovery pulse sequence. The T_2 values were evaluated from the line widths.

1D steady-state NOE experiments have also been carried out with irradiation times ranging between 60 and 100 ms with radio frequency power corresponding to about 30% of reduction in intensity of the irradiated peak. The sequence

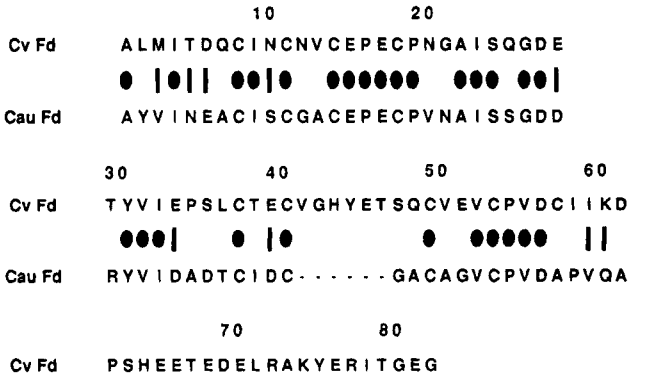

FIGURE 1: Amino acid sequences of Cv Fd (Hase et al., 1977) and Cau Fd (Meyer et al., 1993): filled circles represent identical residues and vertical lines represent residues with a score ⩾1 in the BLOSUM 62 substitution matrix (Henikoff & Henikoff, 1992).

was preceded by a WEFT-type pulse and delay (Patt & Sykes, 1972) to enhance the signal intensity of the fast relaxing signals.

Phase-sensitive TOCSY (Bax & Davis, 1985) and NOESY (Macura et al., 1981) were performed at different temperatures between 289 and 298 K, in the pure absorption mode (States et al., 1982). TOCSY experiments were recorded using a MLEV-17 pulse train of 40 ms typical duration with an effective spin-lock field of 12.5 kHz and surrounded by two 1-ms trim pulses (Bax, 1989). In the case of the detections of downfield-shifted protons, a DIPSI experiment (Shaka et al., 1988) was implemented. In H_2O solvent experiments, a flip-back preceded a jump−return (Guéron et al., 1992) in order to bring back the spins along the z axis. NOESY experiments were performed with mixing times in the 30−150 ms range. The size of the data matrix of 2D experiments was set to 1024 complex points in t_2 and 700 real points in t_1 and 96 transients for each increment, transformed in a 2048 × 1024 data matrix after zero-filling.

For the detection of the downfield-shifted protons in NOESY and TOCSY, a shorter mixing time (10 ms) was used and the recycling delay was made as short as possible, of the order of 250 ms. The number of scans per transient was increased to 800. A WEFT sequence (Patt & Sykes, 1972) with a delay of 32 ms was also used to enhance the paramagnetic shifted signals with respect to the diamagnetic ones. MCOSY (Bax et al., 1981) experiments were performed at 293 K in D_2O. A total of 1024 complex points were recorded with 250 t_1 increments and 3000 transients per increment.

The $^1H-^{13}C$ correlations were obtained with the sequence HMQC (Bax et al., 1983). The emphasis was put on the recycling delay and 2800 transients were added for each t_1 increment.

NMR data were processed on a SUN Sparc station with the Varian software. A low-frequency filter (50 Hz) around the water signal was used as well as optimized sine-bell squared shifted functions.

(c) EPR Spectroscopy. EPR spectra were recorded with a Varian E-109 spectrometer as already described (Moulis et al., 1984).

RESULTS

Sequence-Specific Assignments. A total of 81 spin systems of the expected 82 amino acids composing the Cv Fd sequence (Figure 1) have been observed. In the fingerprint

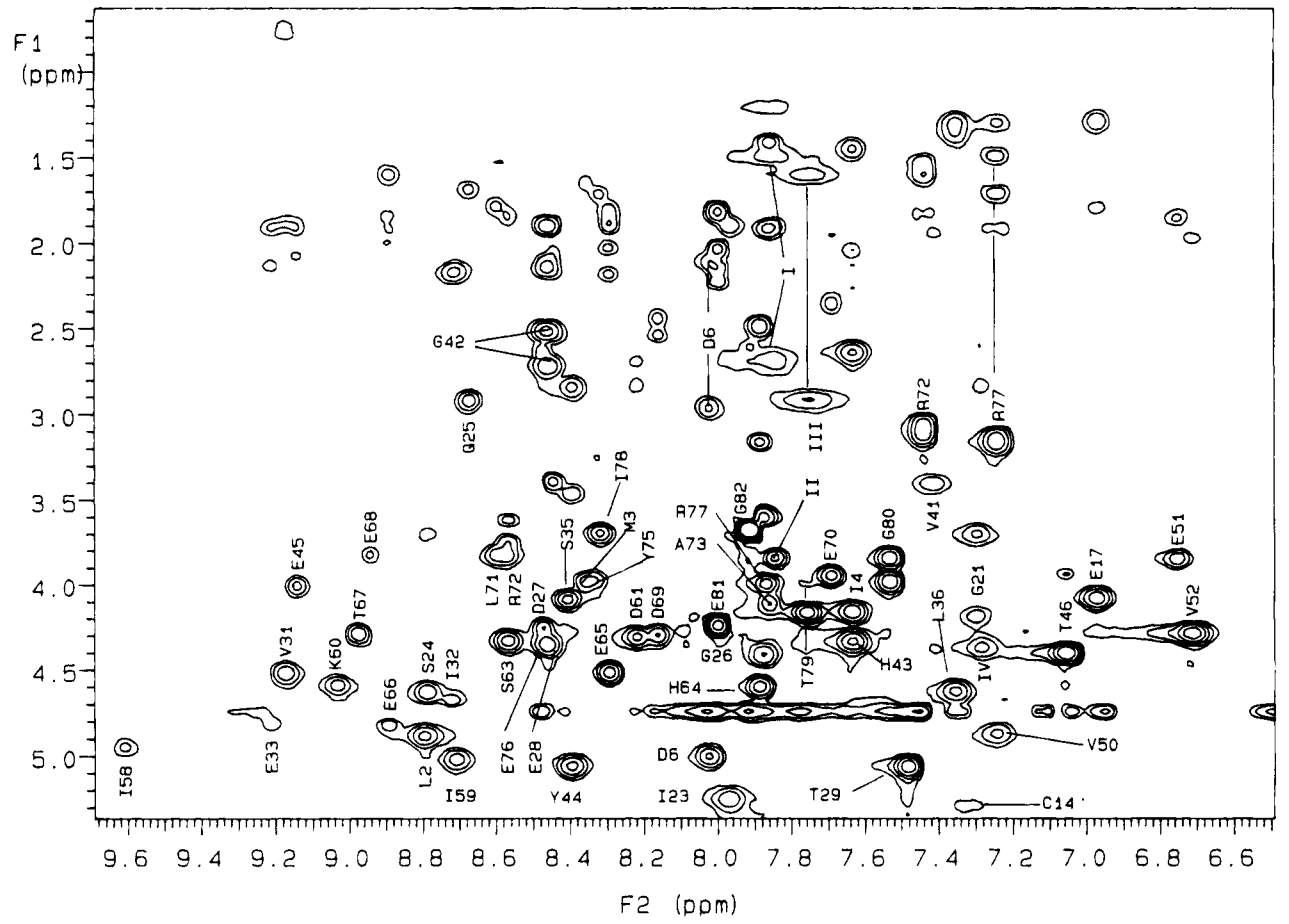

FIGURE 2: Part of the 500-MHz TOCSY spectrum recorded at 293 K showing the fingerprint region of Cv Fd. The experimental conditions are those described under Materials and Methods. The assignments refer to Table 1.

region (Figure 2), the signatures of 55 spin systems were evidenced. The amidic protons of 17 other spin systems have not been detected, while the NH proton only of yet another amino acid appeared in the NOESY spectra. The signals of the eight ligating cysteines were found in specific positions described below.

The sequential assignments were based on the $C_\alpha H_i - NH_{i+1}$ and $NH_i - NH_{i+1}$ NOE connectivities and on those between the side chain protons of residue i with the NH of residue $i+1$ (Wüthrich, 1986). They have been obtained for the amino acids 1−3, 16−17, 23−29, 31−32, 34−36, 41−47, 51−52, and 57−82. Ala-1, the tripeptide 4−6, Ile-9, Gly-21, Tyr-30, and Val-50 were also assigned but by an indirect way (Table 1).

Only nonsequential assignments will be presented. The strong $C_\alpha H-NH$ autocorrelation peak of Leu-2 could overlap a sequential $C_\alpha H-NH$ cross-correlation between Ala-1 and Leu-2. The characteristic $C_\alpha H-C_\beta H$ correlation of an Ala-type spin system in TOCSY and COSY spectra confirmed the assignment of the three N-terminal residues as the unique suitable tripeptide Ala-Leu-Met. Thr-5 and Asp-6 were tentatively attributed, in spite of the lack of sequential correlations, on the basis of $C_\gamma H$(Leu-2)$-C_\alpha H$(Thr-5), $C_\delta H$-(2)$-C_\alpha H(5)$, and $C_\beta H(3)-NH(6)$ connectivities.

All of the main chain protons in the 23−36 segment were also assigned, except for Tyr-30. Connectivities between $C_\alpha H(29)$ and the aromatic protons of Tyr-30 allowed us to partially assign the latter residue, including the β protons on the basis of strong autocorrelations. The 31−32 dipeptide was assigned as described in the discussion and Glu-33 was identified by NOE connectivities between its $C_\alpha H$, $C_\beta H$, and $C_\gamma H$ on one hand and the NH of Ser-35 on the other hand.

A correlation between $C_\gamma H(41)$ and NH(42) helped recognizing Val-41, whereas the cross-correlations $C_\alpha H(41)-NH(42)$ and $C_\beta H(41)-NH(42)$ were hidden by autocorrelations. The only detected proton of Ser-47 was identified by its interactions with $C_\alpha H$, $C_\beta H$, and $C_\gamma H$ of Thr-46. A NOE cross peak between amidic protons of Val-50 and Val-52 ensured the assignment of Val-50.

The stretch encompassing residues 58−61 has three residues with incomplete spin systems. It was assigned by comparison, being the only possible motif constituted by four sequentially related spin systems ended by an AMX (Asp-61) coupling scheme. Cys-57 was assigned on the basis of a connectivity between the $C_\alpha H$ of Cys-57 and the NH of Ile-58. The chemical shifts exhibited by the signals of Cys-57 indicate that this residue is not strongly influenced by the electronic spin of the clusters and point out this Cys as the only nonligating one in the sequence. This is consistent with the sequence alignment (Figure 1).

Conventional sequential assignments revealed the C-terminal end starting from Pro-62. The two final residues, Glu-81 and Gly-82, have resonances with very narrow line widths due to the mobility of this part of the protein. Gly-21 was identified as the last remaining glycine in the sequence.

Fourteen residues, namely, Gln-7, Asn-10, -12 and -20, Val-13 and -55, Glu-15 and -39, Pro-19 and -54, Ala-22,

Table 1: ^{1}H Resonance Assignments of Oxidized Cv Fd and Unassigned Spin Systems[a]

residue	NH	$C_\alpha H$	$C_\beta H$	others
Ala-1[b]		4.88	1.23	
Leu-2	8.79	4.88	2.00	$C_\gamma H$ 0.79; $C_\delta H$ 1.28
Met-3	8.35	3.98	1.95, 1.65	2.08[b]
Ile-4[b]	7.62	4.16	1.45	$C_\gamma H$ 2.16, 2.05
Thr-5[b]		5.68	4.99	1.88[b]
Asp-6[b]	8.02	4.96	2.95, 2.12	
Ile-9				$C_\gamma H$[d] 1.19, 0.98
Pro-16		4.35	2.15, 1.75[c]	$C_\gamma H$ 1.84
Glu-17	6.96	4.08	1.32	$C_\gamma H$ 1.87
Gly-21	7.28	4.18, 3.70		
Ile-23	7.96	5.25	1.90, 1.63[b]	$C_\gamma H$ 1.29, 1.09; $C_\delta H$ 0.36
Ser-24	8.78	4.63	3.72, 3.67	
Gln-25	8.67	2.92	1.30	$C_\gamma H$ 1.69, 1.52; $N_\epsilon H$ 7.12, 6.62
Gly-26	7.87	4.41, 3.60		
Asp-27	8.47	4.26	2.63, 2.53	
Glu-28	8.44	4.35	2.18, 1.91	$C_\gamma H$ 2.11[b]
Thr-29	7.48	5.07	4.17	$C_\gamma H$ 1.14
Tyr-30			3.10, 3.05	$C_{2,6}H$ 7.25; $C_{3,5}H$ 6.77
Val-31	9.17	4.51	1.89	$C_\gamma H$ 0.79, 0.73
Ile-32	8.71	4.68	2.18	$C_\gamma H$ 1.37[b]
Glu-33	9.20	4.81	2.14, 1.92	$C_\gamma H$ 2.41
Pro-34		4.13	1.77, 1.66	$C_\gamma H$ 1.18; $C_\delta H$ 3.84
Ser-35	8.41	4.09	3.84	
Leu-36	7.35	4.62	1.38	$C_\gamma H$ 1.30; $C_\delta H$ 0.80, 0.72
Val-41	7.40	3.41	1.95	$C_\gamma H$ 0.88, 0.72
Gly-42	8.45	2.72, 2.52		
His-43	7.62	4.33	2.64	C_2H 8.07; C_4H 7.08
Tyr-44	8.39	5.06	3.46, 2.84	$C_{2,6}H$ 7.44; $C_{3,5}H$ 6.94
Glu-45	9.14	4.01	2.08, 1.92	$C_\gamma H$ 2.27, 2.21
Thr-46	7.04	4.40	3.94	$C_\gamma H$ 0.89
Ser-47	7.96			
Val-50	7.23	4.87	1.30	$C_\gamma H$ 0.70
Glu-51	6.74	3.85	1.86	
Val-52	6.70	4.28	1.98	$C_\gamma H$ 0.62, 0.37
Cys-57		5.28	2.67	
Ile-58	9.60	4.95	2.16	$C_\gamma H$ 2.00
Ile-59	8.70	5.02	2.17	$C_\gamma H$ 1.37[b]
Lys-60	9.02	4.59	1.26	$C_\gamma H$ 0.81[b]
Asp-61	8.21	4.32	2.84, 2.72	
Pro-62		4.43	2.31	$C_\gamma H$ 2.08, 1.98; $C_\delta H$ 4.30, 4.04
Ser-63	8.56	4.33	3.75, 3.63	
His-64	7.88	4.60	3.17, 2.50	C_2H 8.40; C_4H 7.33
Glu-65	8.28	4.51	1.90, 2.04[c]	$C_\gamma H$ 2.19, 1.82[c]
Glu-66	8.89	4.81	1.85, 1.61	$C_\gamma H$ 2.01, 1.92
Thr-67	8.97	4.28	4.66	$C_\gamma H$ 1.26
Glu-68	8.94	3.82	2.06,[c] 1.93[c]	$C_\gamma H$ 2.22,[c] 2.18[c]
Asp-69	8.16	4.29	2.55, 2.45	
Glu-70	7.68	3.95	2.35, 2.22[c]	$C_\gamma H$ 1.98[c]
Leu-71	8.59	3.82	1.78	$C_\gamma H$ 0.59,[d] 0.53[d]
Arg-72	8.56	3.83	1.87, 1.82	$C_\gamma H$ 1.60, 1.55; $C_\delta H$ 3.12, 3.06; $N_\delta H$ 7.43; $N_\epsilon H$ 6.48
Ala-73	7.85	4.11	1.42	
Lys-74	8.44	3.40	2.05	$C_\delta H$ 2.22;[e] $C_\epsilon H$ 2.58[e]
Tyr-75	8.32	3.97	3.38, 3.25	$C_{2,6}H$ 7.03; $C_{3,5}H$ 5.98
Glu-76	8.45	4.35	2.18, 1.91	2.11[b]
Arg-77	7.83	3.99	1.89, 1.74	$C_\gamma H$ 1.50; $C_\delta H$ 3.16; $N_\delta H$ 7.23
Ile-78	8.31	3.70	1.72	$C_\gamma H$ 0.83; $C_\delta H$ 1.06
Thr-79	7.75	4.16	4.00	$C_\gamma H$ 1.01
Gly-80	7.52	3.98, 3.85		
Glu-81	7.99	4.24	2.04, 1.83	$C_\gamma H$ 2.23, 2.15
Gly-82	7.91	3.68		
Val-x		3.99	2.92	1.61, 1.30
Val-y		3.48	1.96	1.21, 0.93
I[f]	7.84	2.69	1.50	
II	7.83	3.85	1.91	
III[f]	7.75	2.92	1.60	
IV	7.27	4.36	2.86	
V		5.34	3.12	
VI		5.16	2.64	1.16
VII		5.00	2.05	
VIII		4.97	2.35	1.08
IX		4.87	2.44	2.10
X		4.14	3.81	
XI		3.65	1.62	
XII		3.55	2.23	1.98, 1.64, 0.63

[a] Cysteines residues chemical shifts (Cys-57 excepted) are listed in Table 3. Chemical shifts are in ppm at 293 K and pH 6 with an accuracy of 0.02 ppm. [b] Tentative assignments. [c] $C_\beta H$ or $C_\gamma H$. [d] $C_\gamma H$ or $C_\delta H$. [e] $C_\gamma H$, $C_\delta H$, or $C_\epsilon H$. [f] Very broad correlations.

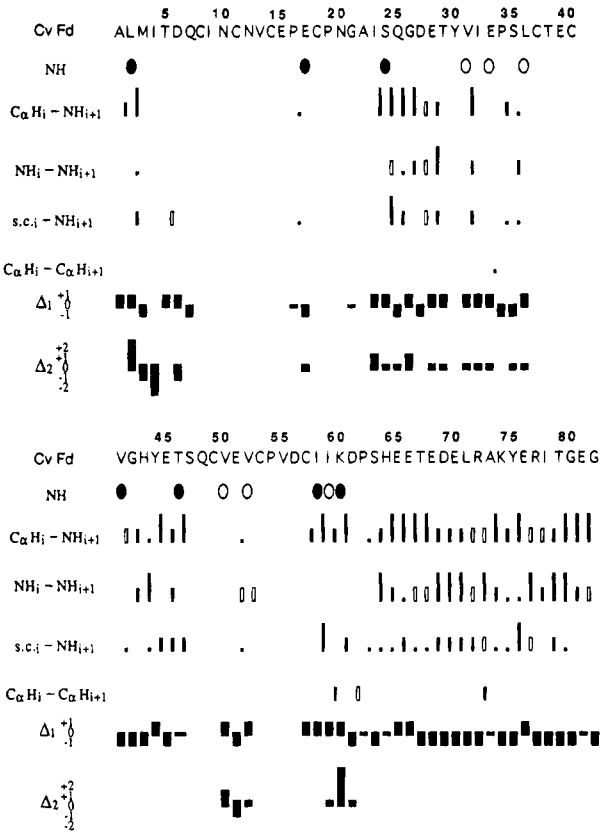

FIGURE 3: Summary of the sequential assignments. (NH) Amidic protons. Empty circles represent the slowly exchangeable protons in both Cau and Cv Fd. Filled circles show exchangeable protons in only Cv Fd. ($C_\alpha H_i - NH_{i+1}$, $NH_i - NH_{i+1}$, s.c.$_i - NH_{i+1}$, and $C_\alpha H_i - C_\alpha H_{i+1}$) Sequential NOEs involving the NH, $C_\alpha H$, and side chain protons. Empty bars correspond to overlapped correlations. The bar height discriminates between strong and weak NOEs. (Δ_1) is the difference between the $C_\alpha H$ chemical shifts of Cv Fd (this work) and those of a random coil (Wishart et al., 1991): +1 and −1 stand for ≥ 0.1 ppm and ≤ -0.1 ppm chemical shift differences, respectively. (Δ_2) Chemical shift differences between the NHs of Cv Fd and Cau Fd after calibration of the shifts against the average chemical shifts of the involved residues (Wishart et al., 1991). ±2, ±1, and 0 stand for shifts differing by more than 1 ppm, by 0.5−1 ppm, and by less than 0.5 ppm, respectively.

Thr-38, Gln-48, and Asp-56, have not been assigned at all. Fourteen remaining spin systems were observed but could not be identified (Table 1). Two of them are characteristic Val-type spin systems, named Val-x and Val-y, which correspond to the remaining valines 13 and 55. In 10 of these 14 spin systems, the amidic protons were not detected. The results are summarized in Table 1.

Labile Proton Exchange. Among the assigned residues, the slowly exchanging amidic protons are those of Leu-2, Glu-17, Ser-24, Val-31, Glu-33, Leu-36, Val-41, Thr-46, Val-50, Val-52, Ile-58, Ile-59, and Lys-60 (Figure 3). The intensities of their signals were stable over 3 weeks at 20 °C. For comparison, the slowly exchanging amidic protons in Cau Fd are those of residues 3, 31, 33, 36, 44, 46, and 53.

Secondary Structure. Most of the secondary structure of Cv Fd in solution can be defined by the preceding results. In the C-terminal part, an α-helix involves 10 residues, namely, from Asp-68 to Arg-77, as identified by the characteristic $NH_i - NH_{i+1}$, $C_\alpha H_i - NH_{i+3}$, $C_\beta H_i - NH_{i+3}$ NOE and the values of the chemical shifts (Figures 3 and 4).

The region between Ile-59 and Glu-65 is folded in such a way that it gives $C_\alpha H(59) - C_\alpha H(62)$ and $C_\alpha H(62) - NH(65)$ NOEs (Table 2). No other NOE between residues i and $i+3$ concerning residues 59−65 has been detected, excluding an α-helix.

The main secondary structural element involving the stretch 41−47 is a turn, as shown by correlations between each proton of Tyr-44 and NH(46) as well as a NOE between $C_\gamma H(41)$ and NH(44).

A number of NOEs, relating various protons of residues 24−27 to protons of residues 29−31 (Table 2), indicate that these two strands run nearly antiparallel. Connectivities between the N-terminal part (namely, Leu-2, Met-3, Ile-4, and Asp-6) and the segment Cys-57−His-64 suggest a rather close spatial contact which will be discussed below. The main detected long-range NOEs are summarized in Table 2.

Cysteinyl Protons: (a) Oxidized Level. The 500-MHz ^{1}H-NMR spectrum of Cv Fd, recorded in D_2O at 20 °C, is shown in Figure 5 (upper trace). Signals to the low-field side of 6.0 ppm originate from three classes of resonances: paramagnetically shifted protons, the ring protons of the Tyr residues 30, 44, and 75 and of the His residues 43 and 64, and the slowly exchanging NH. The shifted resonances are labeled with lowercase letters starting from the most shifted one. The fast relaxing signals can be emphasized by WEFT-type experiments devised to invert or suppress those which have a T_1 larger than 50 ms (Figure 5, lower trace). Every integrated signal corresponds to one proton with the exception of the signal at 10.24 ppm (g, h) which amounts to two. The relaxation times of the most shifted protons are reported on Table 3: they are short but comparable with those measured in other 2[4Fe-4S] Fd (Busse et al., 1991).

The temperature dependence of the shifted signals is anti-Curie. This has been observed for all $[4Fe-4S]^{2+}$ proteins studied so far (Phillips & Poe, 1973) and can be associated with a significant contribution of the excited spin states with $S > 0$ (Gaillard et al., 1987), whereas the ground level is diamagnetic ($S = 0$).

All the experimental results (see also below) on the most shifted signals point to a very close resemblance with those observed in other similar ferredoxins: they are assigned to the $C_\beta H$ of cysteines liganding the clusters.

For the well resolved shifted and fast relaxing protons, through-bond connectivities were evidenced by MCOSY or TOCSY experiments (not shown). Ten signals were connected in pairs: (a, a′), (c, c′), (d, d′), (e, e′), and (f, f′), with the prime attributed to the second, less shifted, proton of a geminal $C_\beta H$ pair.

NOESY experiments using short mixing times (10 ms) confirm and extend the above established spin systems and reveal new ones (Figure 6). The single signal, noted (g, h), which corresponds to two protons, gives correlations with two other signals at 9.06 and 7.69 ppm which were associated with the corresponding g′ and h′. The distinction between $C_\beta H$ protons (those with prime indices) and $C_\alpha H$ protons will be assessed on more definitive grounds when the sequence-specific assignments are discussed. Additional NOE peaks with surrounding residues have also been detected and will be used below for the assignments. Steady-state NOEs were also collected by selectively saturating resonances a through h with irradiation times of 100 ms.

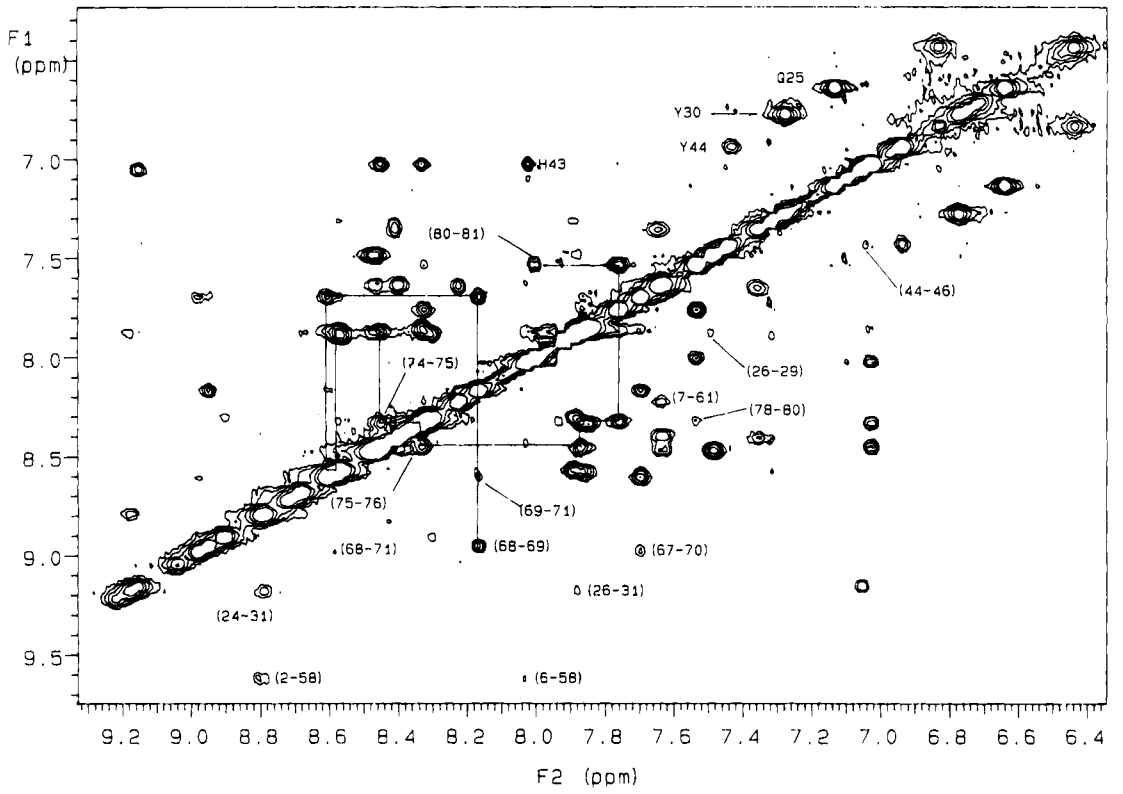

FIGURE 4: Part of the NOESY spectrum recorded at 293 K. A few cross peak assignments have been indicated.

Table 2: Long-Range NOEs

residues 2−6 and 57−64	residues 24−31	other residues
NH(2)−NH(58)	NH(24)−NH(31)	CαH and Cβ H(33)−NH(35)
NH(2)−βH(58)	NH(24)−Cγ H(31)	Cγ H(41)−NH(72)
Cγ H and Cδ H(2)−NH(58)	αH(25)−NH(31)	Cγ H(41)−NH(75)
Cγ H and Cδ H(2)−CαH(5)	NH(26)−NH(29)	C_2H(43)−$C_{2,6}$H(75)
CαH(3)−NH(58)	NH(26)−NH(31)	C_2H(43)−$C_{3,5}$H(75)
Cβ H(3)−NH(6)	NH(26)−Cγ H(31)	C_4H(43)−$C_{2,6}$H(75)
NH, CαH, Cβ H and Cγ H(4)−NH(61)	NH(29)−Cγ H(31)	C_4H(43)−$C_{3,5}$H(75)
NH(6)−CαH(57)		NH, CαH, Cβ H and C_2H(44)−NH(46)
NH(6)−NH(58)		CαH(59)−CαH(62)
CαH and Cβ H(6)−NH(63)		CαH(62)−NH(65)
CαH(6)−NH(64)		NH(66)−Cδ H(71)
Cβ H(6)−C4H(64)		

The results were in agreement with those evidenced by NOESY experiments and will not be commented on further.

Through $^1H-^{13}C$ correlations obtained by HMQC experiments, some of the side chain carbons of the cysteinyl residues have been obtained (Table 3).

(b) Reduced Level. The 1D ^1H NMR spectra of fully reduced samples displayed strongly downfield-shifted signals (Figure 7), with no evidence of residual oxidized ferredoxin, as judged by the disappearence of the signals between 10 and 20 ppm discussed above (Figure 5). Resonances downfield of 25 ppm were expected for ligands of paramagnetic $[4Fe-4S]^+$ clusters, but only six such resonances, each contributed by one proton, were observed (Figure 7), at variance with the higher number of about 13 observed with other 2[4Fe-4S] ferredoxins (Gaillard et al., 1987, 1993b; Bertini et al., 1992, 1994). In addition, two highfield-shifted peaks were detected at −3.22 and −5.83 ppm in Cv Fd (not shown).

An EPR sample examined under identical conditions, i.e., fully reduced, has displayed a single rhombic signal with g values of 2.07, 1.94, and 1.89 amounting to two spins per molecule (Figure 8). The EPR spectra of partially reduced Cv Fd have also been found to display signals very similar to the fully reduced samples; these signals are remarkable by the unusual shape of the $g = 1.94$ line. Overall, no clear evidence of intercluster magnetic interaction has been found in any of these spectra.

Fully reduced Cv Fd is not stable for a very long time in the conditions of the NMR experiments and tends to return to the fully oxidized level. During this process, the hyperfine-shifted signals of oxidized ferredoxin between 10 and 20 ppm (Figure 5) reappeared concomitantly, at the expense of the disappearing resonances of reduced ferredoxin (Figure 7), but no additional peaks which could arise from semireduced ferredoxin have been observed. Accordingly, an EXSY experiment carried out on a partially reduced sample with a mixing time of 3 ms failed to provide any correlation between the signals associated with the same proton of the oxidized and reduced protein.

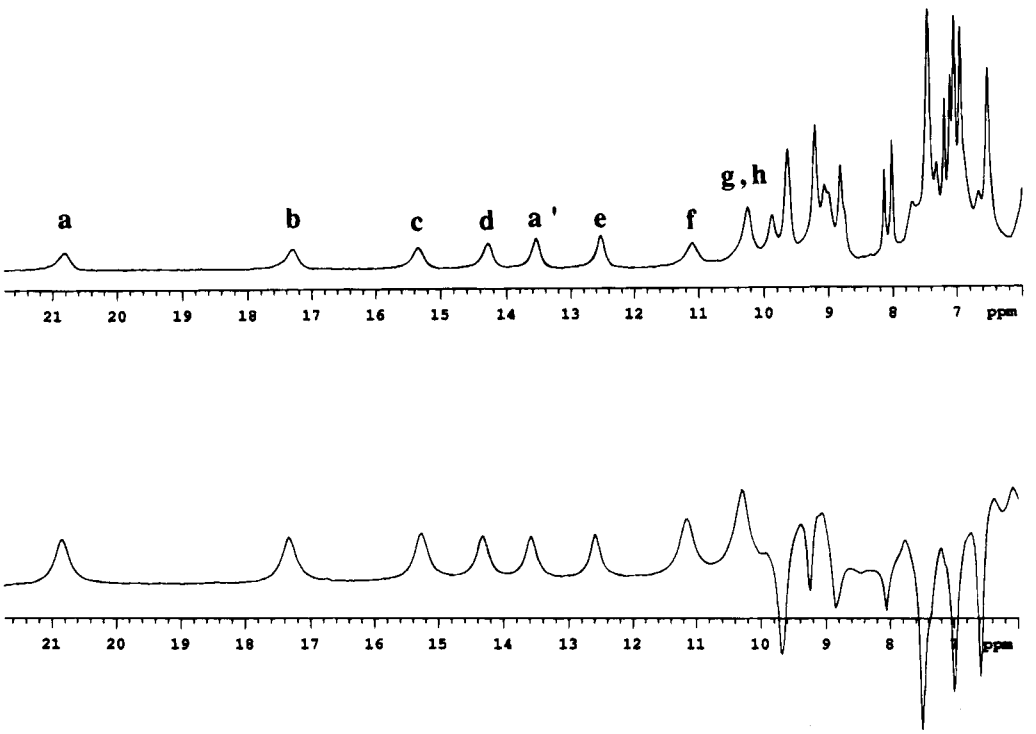

FIGURE 5: Downfield part of the ^{1}H NMR spectra of oxidized Cv Fd. (Upper trace) Obtained with a selective presaturation of water followed by a nonselective 90° pulse. (Lower trace) Obtained with the sequence 180°−32-ms delay−90° with selective irradiation of water during the 32-ms delay. The slowly relaxing signals with $T_1 \geq 50$ ms have been inverted or suppressed.

DISCUSSION

Despite the significant differences between the primary structures of short 2[4Fe-4S] Fd and of Cv Fd (Figure 1), the present sequence-specific assignments strongly indicate that many structural features of the latter protein resemble those of the former. For instance, the comparison of the chemical shifts in the region of amino acids 23−30 between Cp Fd (Gaillard et al., 1993a) and Cv Fd (Table 1) shows that this part of the two molecules folds in a very similar way. Two spin systems occur in positions which are very similar to those of the signals associated with Val-31 and Ile-32 in Cp and Cau Fd (Gaillard et al., 1993a) and are assigned to these same residues in Cv Fd. The common set of slowly exchanging protons associated with residues 31, 33, and 36 confirms the similar fold of all three ferredoxins, in at least the region spanning residues 23−36.

Unassigned residues of Cv Fd occur in the regions which have escaped detection in the cases of Cp and Cau Fd (Gaillard et al., 1993a). These involve the dipeptides separating two consecutive cysteine ligands (i.e., positions 9, 10, 12, 13, 38, and 39), as well as the amino acids following the Cys-Pro sequence serving as the remote ligand of the clusters (in positions 20−22 for cluster II and 54−56 for cluster I). Gly-21 of Cv Fd was assigned because it was the last spin system for a Gly residue left, but the identification of the amino acid in this position usually relies on specific experiments (Gaillard et al., 1993b; Quinkal et al., 1994). Indeed, the spin systems associated with these residues can generally be observed, but their amidic protons usually escape detection which eludes sequential NOE connectivities. The reasons for these difficulties have already been discussed (Gaillard et al., 1992, 1993a); they arise from the short distance between these protons and the clusters and from the building of hydrogen bonds between most of these protons and the sulfur atoms of the [4Fe-4S] complexes (Backes et al., 1991; Duée et al., 1994). The similar pattern of unassigned residues displayed by short 2[4Fe-4S] Fd (Gaillard et al., 1993a) and Cv Fd then implies that the network of hydrogen bonds around the clusters is fairly well conserved among all of these proteins, despite the larger size of the latter one.

Considering the unique features of Cv Fd, as compared to shorter 2[4Fe-4S] Fd (Figure 1), the six residues insertion between Cys-40 and Cys-49 has been totally assigned, except for its last residue (Gln-48); this may be taken as an indication that these additional amino acids do not stay close to the clusters and point outward as a loop, with a turn around residue 45 which brings Tyr-44 in close proximity to the main chain of Thr-46. Only Ser-47 and Gln-48 appear to be perturbed by the cluster, much like the dipeptide separating the other ligands (see above). In addition, this part of the molecule may interact with a region of the C-terminus as witnessed by the NOEs between the NH of Arg-72 and Tyr-75 and protons of Val-41 and His-43 (Table 3).

The C-terminal 22 amino acids of Cv Fd do not display homology to other well characterized ferredoxins. This region could be conventionally assigned, which indicates that this part of the protein does not sense the electronic spin of the clusters. Its most remarkable element is an α-helix spanning residues 68−78: a considerable amount of experimental evidence (Figure 3) supports the presence of this helical structure, and the last amino acid (Ile-78) was included on the basis of the upfield chemical shift of its C_α proton compared to an average value (Wishart et al., 1991). $C_\alpha H(79)$ displays a similarly upfield-shifted value, but it was not added to the helix due to the lack of correlation between its amidic proton and $C_\alpha H(76)$.

Table 3: ^{1}H NMR Assignments for Cysteines of Cv Fd

Cys	cluster type	peaks	δ (ppm)	δ_h[a] (ppm)	θ[b]	T_1 (ms)	T_2 (ms)
8	I	f	11.09	8.09	−57.69	5.6	3.3
		f′	9.88	6.88	−175.00	14.9	7
		H_α	7.36			*c*	*c*
		C_β	124.0[d]				
		C_α	119.1[e]				
11	I	c	15.36	12.36	59.00	6.7	3.4
		c′	8.98	5.98	176.00	11.8	<10
		H_α	9.64			*c*	*c*
		C_β	125.2				
14	I	d	14.28	11.28	132.00	8.3	4.1
		d′	5.22	2.22	13.00	*c*	*c*
		H_α	7.33			*c*	*c*
		C_α	119.1[e]				
53	I	e	12.52	9.52	−161.00	8.7	5.1
		e′	5.66	2.26	−41.00	*c*	<16
		H_α	7.37			*c*	*c*
18	II	h	10.24	7.24	−162.00	9.4	~5
		h′	7.69	4.69	−42.57	12.1	4.8
		H_α	4.36 or 3.44			*c*	*c*
		C_β	124.8 or 124.3				
37	II	g	10.24	7.24	−56.70	9.4	~5
		g′	9.06	6.06	−175.00	13.0	<13
		H_α	3.44 or 4.36			*c*	*c*
		C_β	124.3 or 124.8				
40	II	a	20.84	17.84	62.70	7.1	3.4
		a′	13.54	10.54	178.40	9.8	4.7
49	II	b	17.27	14.27	135.10	7.3	3.3
		b′	4.00	1.00	17.00	*c*	~13
		H_α	6.82			*c*	*c*
		C_α	122.0				

[a] Hyperfine shifts which have been estimated by subtracting 3.0 ppm from the experimental chemical shifts. This value represents the averaged chemical shift of $C_\beta H$ cysteines coordinated either to Zn (Blake et al., 1991) or to Cd (Henehan et al., 1993) in substituted rubredoxins. [b] Dihedral angles Fe-S-C_β—H_β (deg) of corresponding cysteines from Cau Fd (Duée et al., 1994). [c] Signals overlapped in crowded areas. [d] Chemical shifts of ^{13}C are referenced to DSS. [e] Attributed to C_α Cys-8 or Cys-14.

It has already been shown that correlations between protons of the N-terminal and of the C-terminal parts of Cp and Cau Fd (Gaillard et al., 1993a) can be observed, in agreement with X-ray crystallographic results attributing an important stabilizing role to the proximity of these two strands (Duée et al., 1994). In the case of Cv Fd, a few long-range NOEs have been observed between protons of N-terminal residues and protons of the 58−64 segment (Table 2), but the pattern does not exactly correspond to that observed with equivalent residues (Figure 1) of Cp and Cau Fd (Gaillard et al., 1993a). Similarly, the set of slowly exchanging NH of Cv Fd differs from that of Cau Fd for those residues belonging to the N-terminus and for residues 53−55 of Cau Fd and 59−62 of Cv Fd. It can then be concluded that the presence of a long C-terminal tail in Cv Fd changes the interaction between the two parts of the Cv Fd molecule that correspond to the N- and C-termini of short 2[4Fe-4S] Fd and may contribute to other stabilizing effects like the close contact exhibited between residues 41−43 and 72−75.

Sequence-Specific Assignments of Cysteines. The correspondence between hyperfine-shifted signals of [4Fe-4S] proteins and the exact amino acids giving rise to them has long been a difficult task due to the very short relaxation times of these protons which impeded the detection of sequence-specific NOEs. It has early been recognized that most resonances occurring at lower field than 10 ppm are attributable to protons of the cysteine ligands of the cluster (Packer et al., 1977). Since then, various attempts have aimed at assigning these signals, mainly in the case of Cp Fd (Busse et al., 1991; Bertini et al., 1992). Very recently, two experimental approaches have been instrumental in affording a consistent set of assignments for these unusual signals: one consisting in slightly modifying the immediate environment of the clusters (Gaillard et al., 1993b),[2] the other combining the observation of long-range correlations and the likeliness of their occurrence based on X-ray crystallographic results (Bertini et al., 1994). Since none of these approaches can yet be implemented for Cv Fd, the following discussion relies on the partial similarity in the folding of Cau Fd and Cv Fd demonstrated above and on the pattern observed in the case of Cp and Cau Fd.

From a combination of 1D and 2D NMR experiments, eight spin systems have been identified (Table 3) which correspond to the side chains of the eight cysteine residues connecting the two [4Fe-4S] clusters to the main chain of Cv Fd.

Both signals f and f′ have NOEs with resonances at 4.17 and 1.14 ppm associated with Thr-29 (Table 1). The crystal structure of Cau Fd predicts a close contact between Cys-8 and the residue in position 29. Signals f and f′ are thus assigned to Cys-8. Furthermore, Ile-4 was tentatively assigned on the basis of a correlation between f and one of its side chain proton.

NOEs are detected between c and signals at 1.19 and 0.98 ppm, corresponding to side-chain protons of an unassigned long-chain residue. The situation is reminiscent of the NOEs observed between the signal of one $C_\beta H$ of Cys-11 and those of side-chain protons of Ile-9 in Cau Fd (Bertini et al., 1994). Similarly, signals c and c′ may belong to Cys-11 in Cv Fd with c displaying NOEs to $C_\gamma H$ and $C_\delta H$ of Ile-9.

Signal b exhibits a NOE to signal d (Figure 6). This very peculiar interaction is the signature of $C_\beta H$ protons of Cys-43 and Cys-14 in Cau Fd (Bertini et al., 1994) because they are the only $C_\beta H$ protons of cysteines in close contact (Duée et al., 1994). By analogy with Cau Fd, signals b and b′ are assigned to Cys-49 in Cv Fd and d and d′ are assigned to Cys-14. Furthermore, d and the signal of $C_\alpha H$(Cys-49) are connected through a weak NOE. The assignment is further supported by a NOE pattern similar to that observed in Cau Fd (Bertini et al., 1994): a cross peak connects b with a signal at 1.23 ppm, which could be attributed to $C_\gamma H$ protons of Ile-23, and two cross peaks involving d occur at 0.37 ($C_\gamma H$ of Val-52) and 0.21 ppm (most probably $C_\delta H$ of Ile-23).

A NOE between the single degenerate peak labeled (g, h) and a signal at 1.23 ppm reflects the interaction between one $C_\beta H$ proton of Cys-18 with a $C_\gamma H$ of Ile-23, in much the same way as in Cau Fd (Bertini et al., 1994). Two other NOEs between (g, h) and peaks at 4.36 and 3.44 ppm

[2] Tentative assignments of the down field signals in Cp Fd (Gaillard et al., 1993b) were mainly based on the shifts induced by Pro-19 or Pro-48 replacements. Additional data obtained with a modified form in which Asp-39 had been replaced by Ala have more clearly indicated that signal a (Gaillard et al., 1993b) should be assigned to $C_\beta H$ of Cys-40 and, consequently, signals f, c and e to $C_\beta H$ of Cys-18, Cys-11, and Cys-47, respectively, in agreement with recent results (Bertini et al., 1994). However, the shifts of the signals associated with Cys-11 protons (cluster I) upon Pro-19 (cluster II) replacement remain to be explained, as well as the symmetrical ones involving Cys-40 protons upon Pro-48 replacement.

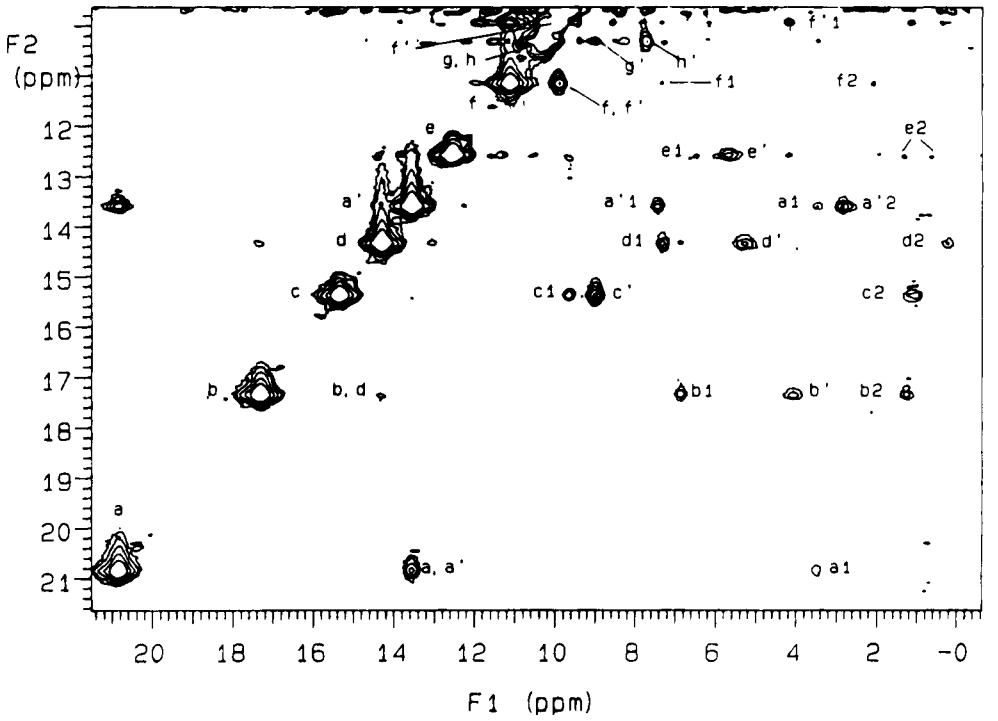

FIGURE 6: Lowfield part of the NOESY spectrum of oxidized Cv Fd recorded at 293 K with a mixing time of 10 ms. The most downfield-shifted $C_\beta H$'s of each cysteinyl residue liganding the clusters are labeled with lowercase letters from a to h, and the geminal proton is designated with the same primed letter. The correlations were attributed as follows: a1, (a, $C_\beta H(44)$); b1, (b, $C_\alpha H(49)$); b2, (b, $C_\gamma H(23)$); c1, (c, $C_\alpha H(11)$); c2, (c, $C_\delta H(9)$); d1, (d, $C_\alpha H(14)$); d2, (d, $C_\delta H(23)$); a'1, (a', $C_{2,6}H(44)$); a'2, (a', $C_\beta H(44)$); (e, $C_\gamma H(50)$); f1, (f, $C_\alpha H(8)$); f2, (f, $C_\gamma H(4)$); f'1, (f, $C_\beta H(29)$).

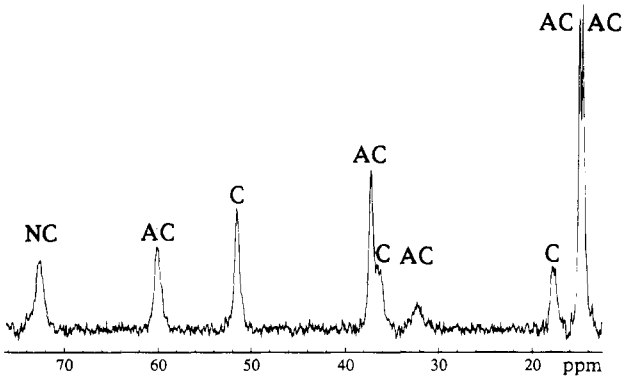

FIGURE 7: Downfield part of the ^1H NMR spectrum recorded at 293 K with reduced Cv Fd in H_2O. The temperature dependence of the signals between 287 and 300 K is indicated with C standing for Curie, AC for anti-Curie, and NC for no temperature dependence. The broad line at −5.23 ppm (not shown) has a Curie temperature dependence.

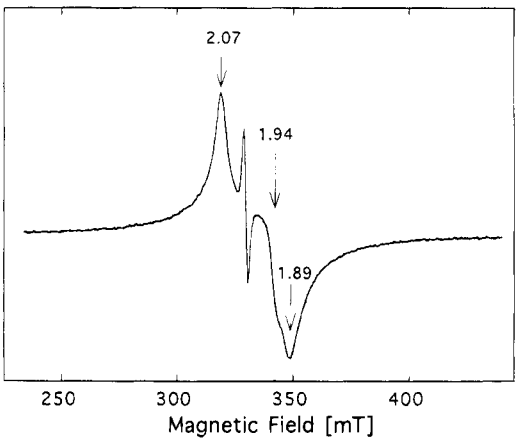

FIGURE 8: EPR spectrum of reduced Cv Fd at 10 K. The sample is the same used above for the NMR experiment of Figure 7. Experimental conditions: microwave frequency, 9.226 GHz; modulation frequency, 100 kHz; modulation amplitude, 1 mT; and microwave power, 0.1 mW. The isotropic signal at $g = 2.00$ is contributed by the viologen radical.

probably result from intraresidue interactions with the $C_\alpha H$ protons of the same cysteines (Table 3).

A situation unlike the one observed with Cau or Cp Fd occurs for signal a', which is strongly interacting with Tyr-44 through two $C_\beta H$ at 2.84 and 3.46 ppm and the ortho protons at 7.44 ppm. Steady-state NOEs have also been evidenced between a and the ortho protons of Tyr-44, and between a' and the meta protons of Tyr-44 at 6.94 ppm on one hand and one $C_\beta H$ of His-43 at 2.64 ppm on the other hand. The (a, a') pair is located down field of 10 ppm, a singular situation in the $2[4Fe\text{-}4S]^{2+}$ proteins studied so far by NMR. These features identify a and a' as the $C_\beta H$ of Cys-40, in agreement with the expected modifications on this particular residue induced by the neighboring insertion when compared to shorter Fd (Figure 1).

Signal e exhibits NOEs at 1.30 and 0.70 ppm, positions which correspond to Val-50 (Table 1). At this stage, two cysteine residues (37 and 53) remain to be assigned. No definite argument allow us to choose between the alternate possibilities, but the values of the chemical shifts of e and (g, h) fall close to those assigned to Cys-47 and Cys-37, respectively, in Cau Fd (Bertini et al., 1994). By analogy, we propose that e and e' arise from the $C_\beta H$ of Cys-53 and the remaining signal of the degenerate doublet from one of Cys-37 (Table 3). It will be shown below that the latter assignments, whereas they are not sustained by enough experimental evidence, agree with the conclusions drawn

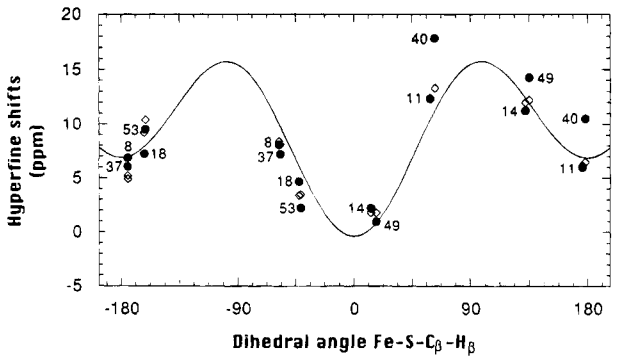

FIGURE 9: Plot of the cysteine $C_\beta H$ hyperfine shifts of Cv Fd (full circles) and of Cau Fd (open squares) versus the corresponding Cau Fd Fe-S-C_β-H dihedral angles (Duée et al., 1994). The line represents the analytical expression (see text) obtained with Cau Fd data. The Cau Fd NMR data are taken from Bertini et al. (1994).

from the other assignments based above on more conclusive grounds.

Similar patterns of long range NOEs involving protons of residues 9, 23, and 29 have been evidenced in both Cau and Cv Fd for the $C_\beta H$ of Cys-8, -11, -14, -18, and -49 (Cv Fd) or -43 (Cau Fd). In contrast, differences between the two proteins have been observed for the NOEs displayed by two cysteines: Cys-40 of Cau and Cv Fd, on one hand, and Cys-53 of Cv Fd and Cys-47 of Cau Fd, on the other hand. Such discrepancies must be associated with a change of structure between the two proteins in the vicinity of the clusters.

Angular Dependence of Paramagnetic Shifts. Recent NMR studies on $[4Fe\text{-}4S]^{3+}$ model compounds (Mouesca et al., 1993) and $[4Fe\text{-}4S]^{2+}$ proteins (Bertini et al., 1994) have established that the isotropic hyperfine interaction of protons on the closest carbon to the iron is a function of the dihedral angle θ defined by the four H-C-S-Fe atoms. In the case of $[4Fe\text{-}4S]^{2+}$ proteins, the paramagnetic shifts (δ) of Cau Fd cysteinyl β-protons (and C_α) have been plotted against the dihedral angles derived from the X-ray crystal structure of Pas Fd (Bertini et al., 1994). We have slightly improved this procedure by using the crystal structure of Cau Fd (Duée et al., 1994) and an only marginally modified empirical law has been obtained by least-squares fitting (Figure 9):

$$\delta = 12.2 \sin^2 \theta - 3.6 \cos \theta + 3.1 \qquad (1)$$

If the same dihedral angles are assumed for Cv and Cau Fd, the chemical shifts of the β-cysteinyl protons of Cv Fd, after subtracting the diamagnetic contribution (set to an average value of 3.0 ppm), can be plotted on Figure 9. It appears that the agreement is fairly good for most protons. The only significant exception is for signals assigned to Cys-40; they display large deviations along the hyperfine shift axis indicating that they will not fit to the curve by a mere variation of θ. Indeed the β-protons of Cys-40 are the only ones, among cysteinyl protons of $[4Fe\text{-}4S]^{2+}$ Fd characterized so far, to occur *both* below 10 ppm. That a change affects Cys-40 on going from Cau Fd to Cv Fd is also apparent from the value of the chemical shift of the $C_\alpha H$: this proton is the only one which has not been detected, implying that it does probably not fall around 10 ppm, unlike in Cau Fd (Bertini et al., 1994). These data on signals associated with Cys-40 may be reconciled if extra spin density is assumed on the sulfur atom of the residue: the perturbation must be local rather than resulting from a global change in the electronic structure of the $[4Fe\text{-}4S]^{2+}$ cluster since the hyperfine shifts associated with the other ligands of the same cluster are almost unchanged between Cau and Cv Fd (Figure 9 and Table 3). One may then consider two contributing factors to the peculiarities of Cys-40. First, the additional amino acids between Cys-40 and Cys-49 may induce a slight structural change on Cys-40 resulting in an enhanced transfer of spin density from the inorganic core to this specific ligand. Second, NOEs have been detected between the pair (a, a′) assigned to the $C_\beta H$ of Cys-40 and several signals associated with Tyr-44 (see above); therefore, the occurrence of ring currents contributed by the nearby aromatic residue may also shift the signals of $C_\beta H(40)$. More data will be required to assess the relative contributions of these effects, but it is already worth noticing that the so far general law used in Figure 9 can fail in some cases where the immediate environment exerts a strong influence on the ligand. Care should be taken in applying the empirical law of Figure 9 to $[4Fe\text{-}4S]^{2+}$ proteins even more atypical than Cv Fd.

However, the noteworthy exception of Cys-40 set aside, the ligands of Cv Fd have the signals of their protons in excellent agreement with the plot of Figure 9. Therefore, the angular dependence of the cysteinyl $C_\beta H$ paramagnetic shifts can be used to clarify some remaining ambiguities in the interpretation of the NMR data and to stereospecifically assign the $C_\beta H$ resonances. The $C_\beta H - C_\beta H$ and $C_\beta H - C_\alpha H$ connectivities are generally distinguished by taking into account the relative intensities and positions and by comparing the relaxation times of the correlated peaks. But, in case of any remaining doubt, eq 1 may be of some help. For example, peak b has two NOE cross peaks with resonances at 6.82 and 4.00 ppm (Figure 6). The cross peak at 4.00 ppm was definitively assigned to the geminal b′ proton because its position better fits the curve of Figure 9 and then, the signal at 6.82 ppm was assigned to the corresponding $C_\alpha H$. In a similar way, the signals corresponding to the second β-proton of Cys-37 and Cys-18 were identified. Examination of Figure 9 shows that a better agreement is obtained if signal h′ (at 7.69 ppm) is assigned to Cys-18 and, consequently, signal g′ (at 9.06 ppm) is assigned to Cys-37.

The stereospecific assignments of the two β-protons of liganding cysteines have already been discussed (Busse et al., 1991). They were based on the values of the relaxation times and on the ratio of the paramagnetic shifts of the signals. Such a method, as established by others (Bertini et al., 1994), has partly failed in the case of Cp Fd. In the case of Cau Fd, the C_β protons closest to the nearby iron atom have the dihedral angle with the smallest absolute value and are the most shifted (Bertini et al., 1994; Table 3) for Cys-8, -11, -37, and -40. For Cys-14, -18, -43, and -47, the C_β protons farthest from the iron atom are the most shifted (Table 3). Therefore, there is no direct relationship between the value of the chemical shift and the closeness of the bound Fe atom for these C_β protons. In the case of Cv Fd, the excellent fit of the paramagnetic shifts to the curve of Figure 9 indicates that the relative orientations of the cysteines $C_\beta H$ are identical to those of Cau Fd.

The Mechanism of Electron Exchange in Cv Fd. In the documented cases of short 2[4Fe-4S] Fd (Phillips & Poe, 1973; Gaillard et al., 1987; Bertini et al., 1992, 1994), the scheme of Figure 10 has been shown to apply to the redox mechanism of these proteins. The steps involving the

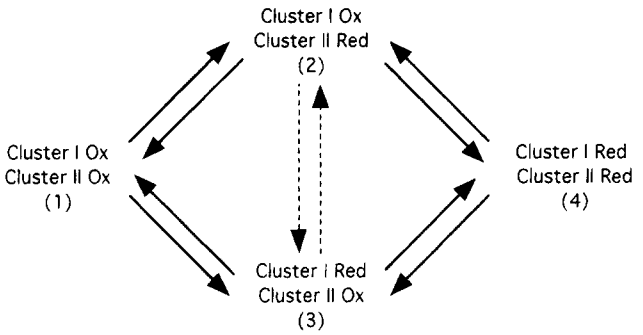

FIGURE 10: Schematic representation of the different redox levels in 2[4Fe-4S]$^{2+/+}$ Fd. All equilibria are detected in Cp and Cau Fd. Only the equilibria indicated by solid line arrows have been observed in Cv Fd.

addition or loss of electrons to or from the protein, (1) ↔ (2) ↔ (4) and (1) ↔ (3) ↔ (4), are slow on the NMR time scale, while intramolecular electron hopping between the clusters, (2) ↔ (3), is fast. As a result, partially reduced samples exhibit NMR broad peaks intermediate between signals of cysteines $C_\beta H$ arising from the fully reduced and the fully oxidized Fd (Gaillard et al., 1987, 1993b; Bertini et al., 1994).

A very different situation holds for Cv Fd. In a variety of partially reduced samples, no intermediate peaks between the signals of oxidized and reduced protein have been detected and no EXSY correlations evidenced among them. Consequently, the strategy which proved beneficial to the assignments of the reduced Fd of Cau and Cp (Bertini et al., 1994) could not be implemented for Cv Fd. Indeed, the fast (2) ↔ (3) exchange prevailing in the short 2[4Fe-4S] Fd does not take place in Cv Fd in the conditions of our experiment. These data provide the unprecedented demonstration of slow or nonexistent intramolecular electron exchange in a Fd where the two [4Fe-4S] clusters are linked by two CysXXXCys pentapeptides (Figure 1). It is unlikely that this change is due to a significant difference between the reduction potentials of the two clusters, since signals assigned to ligands of both oxidized cluster I and cluster II develop at the same time when a fully reduced sample is slowly reoxidizing. One may then conclude that a kinetic barrier prevents the fast electron jump between the two centers of the same Cv Fd molecule, in contrast to the situation evidenced by short 2[4Fe-4S] Fd.

The origin of the decreased rate of intramolecular electron exchange between the two clusters of Cv Fd may be sought in differences associated with the protein structure in the internal core of the molecule. However, no drastic structural change, compared to short Fd (Gaillard et al., 1993a), has been evidenced above for the oxidized proteins in the region linking the two clusters. Then, an explanation involving a difference in the electronic structures of the reduced clusters between Cv Fd and shorter 2[4Fe-4S] Fd could be considered; the occurrence of differences is indeed borne out by both the singular pattern of NMR lines displayed by reduced Cv Fd (Figure 7) and the unusual shape, with little or no magnetic interaction, of the EPR spectra (Figure 8). It may well be that the distribution of the mixed-valence pair (Fe^{2+}–Fe^{3+}) on one or both of the reduced clusters in Cv Fd is different from that in Cp or Cau Fd and impedes both the strong magnetic interaction and the fast electron exchange evidenced in the latter proteins. The localization of the added electron in [4Fe-4S]$^+$ clusters may be seen as a symmetry breaking of the local structure, which most likely depends on the environment of these inorganic cores in proteins. The insertion between cysteines 40 and 49 in the Cv Fd sequence, which has been shown above to interact primarily with cluster II, could change the electronic properties of the nearby cluster. If such an explanation is confirmed, it would be one of the first examples where the detailed electronic structure of the donor and acceptor metallic centers has a direct influence on the rate of electron transfer between them.

Finally, these NMR studies show that Cau Fd and Cv Fd do share a common structural framework over those parts of the sequences that can be aligned. The similarity extends to most of the vicinity of the active centers as judged by the properties of the hyperfine-shifted signals assigned to the protons of liganding cysteines. Still, the intramolecular electron transfer process followed by NMR is remarkably different in Cv Fd than in Cau Fd. Since the redox partners of Fd in Cv are not yet known with certainty, it is difficult to assess whether these differences have a functional bearing. However, this work exemplifies that electron exchange in 2[4Fe-4S] Fd is very finely tuned, and the contributing factors modulating the rates of Figure 10 require further study.

ACKNOWLEDGMENT

We are grateful to Dr. J. Meyer for careful reading of the manuscript. We thank Dr. J.-M. Mouesca for clarifying discussions on spin density distribution. M. Massines is also thanked for her help in HMQC spectra analysis.

REFERENCES

Adman, E. T., Sieker, L. C., & Jensen, L. H. (1973) *J. Biol. Chem. 248*, 3987–3996.

Adman, E. T., Sieker, L. C., & Jensen, L. H. (1976) *J. Biol. Chem. 251*, 3801–3806.

Bachofen, R., & Arnon, D. I. (1966) *Biochim. Biophys. Acta 120*, 259–265.

Backes, G., Mino, Y., Loehr, T. M., Meyer, T. E., Cusanovich, M. A., Sweeney, W. V., Adman, E. T., & Sanders-Loehr, J. (1991) *J. Am. Chem. Soc. 113*, 2055–2064.

Bax, A. (1989) *Methods Enzymol. 176*, pp 151–168.

Bax, A., & Davis, D. G. (1985) *J. Magn. Reson. 65*, 355–360.

Bax, A., Freeman, R., & Morris, G. J. (1981) *J. Magn. Res. 42*, 164–168.

Bax, A., Griffey, R. H., & Hawkins, B. L. (1983) *J. Am. Chem. Soc. 105*, 7188–7190.

Bertini, I., Briganti, F., Luchinat, C., Messori, L., Monnanni, R., Scozzafava, A., & Vallini, G. (1992) *Eur. J. Biochem. 204*, 831–839.

Bertini, I., Capozzi, F., Luchinat, C., Piccioli, M., & Vila, A. J. (1994) *J. Am. Chem. Soc. 116*, 651–660.

Blake, P. R., Park, J.-B., Bryant, F. O., Aono, S., Magnuson, J. K., Eccleston, E., Howard, J. B., Summers, M. F., & Adams, M. W. W. (1991) *Biochemistry 30*, 10885–10895.

Busse, S. C., La Mar, G. N., & Howard, J. B. (1991) *J. Biol. Chem. 266*, 23714–23723.

Cammack, R. (1992) *Adv. Inorg. Chem. 38*, 281–322.

Duée, E. D., Fanchon, E., Vicat, J., Sieker, L. C., Meyer, J., & Moulis J.-M. (1994) *J. Mol. Biol. 243*, 683–695.

Eck, R. V., & Dayhoff, M. O. (1966) *Science 152*, 363–366.

Gaillard, J., Moulis, J.-M., & Meyer, J. (1987) *Inorg. Chem. 26*, 320–324.

Gaillard, J., Albrand, J.-P., Moulis, J.-M., & Wemmer, D. E. (1992) *Biochemistry 31*, 5632–5639.

Gaillard, J., Moulis, J.-M., Kümmerle, R., & Meyer, J. (1993a) *Magn. Res. Chem. 31*, S27−S33.
Gaillard, J., Quinkal, I., & Moulis, J.-M. (1993b) *Biochemistry 32*, 9881−9887.
Guéron, M., Plateau, P., Kettani, A., & Decorps, M. (1992) *J. Magn. Reson. 96*, 541−550.
Hase, T., Matsubara, H., & Evans, M. C. W. (1977) *J. Biochem. (Tokyo) 81*, 1745−1749.
Henehan, C. J., Pountney, D. L., Zerbe, O., & Vasák, M. (1993) *Protein Sci. 2*, 1756−1764.
Henikoff, S., & Henikoff, J. G. (1992) *Proc. Natl. Acad. Sci. U.S.A. 89*, 10915−10919.
Macura, S., Hyang, Y., Suter, D., & Ernst, R. R. (1981) *J. Magn. Reson. 43*, 259−281.
Matsubara, H., & Saeki, K. (1992) *Adv. Inorg. Chem. 38*, 223−280.
Meyer, J., Moulis, J.-M., Scherrer, N., Gagnon, J., & Ulrich, J. (1993) *Biochem. J. 294*, 622−623.
Mouesca, J.-M., Rius, G., & Lamotte, B. (1993) *J. Am. Chem. Soc. 115*, 4714−4731.
Moulis, J.-M., Auric, P., Gaillard, J., & Meyer, J. (1984) *J. Biol. Chem. 259*, 11396−11402.
Nettesheim, D. G., Harder, S. R., Feinberg, B. A., & Otvos, J. D. (1992) *Biochemistry 31*, 1234−1244.
Otaka, E., & Ooi, T. (1987) *J. Mol. Evol. 26*, 257−267.
Packer, E. L., Sweeney, W. V., Rabinowitz, J. C., Sternlicht, H., & Shaw, E. N. (1977) *J. Biol. Chem. 252*, 2245−2253.
Patt, S. L., & Sykes, B. D. (1972) *J. Chem. Phys. 56*, 3182−3184.
Phillips, W. D., & Poe, M. (1973) in *Iron−Sulfur Proteins* (Lovenberg, W., Ed.) Vol. II, pp 255−285, Academic Press, New York.
Plateau, P., & Guéron, M. (1982) *J. Am. Chem. Soc. 104*, 7310−7311.
Quinkal, I., Davasse, V., Gaillard, J., & Moulis, J.-M. (1994) *Protein Eng. 7*, 681−687.
Saeki, K., Suetsugu, Y., Tokuda, K., Miyatake, Y., Young, D. A., Marrs, B. L., & Matsubara, T. (1991) *J. Biol. Chem. 266*, 12889−12895.
Schmehl, M., Jahn, A., Meyer zu Vilsendorf, A., Hennecke, S., Masepohl, B., Schuppler, M., Marxer, M., Oelze, J., & Klipp, W. (1993) *Mol. Gen. Genet. 241*, 602−615.
Shaka, A. J., Lee, C. J., & Pines, A. (1988) *J. Magn. Reson. 77*, 274−293.
Smith, E. T., & Feinberg, B. A. (1990) *J. Biol. Chem. 265*, 5125−5128.
States, D. J., Haberkon, R. A., & Ruben, D. J. (1982) *J. Magn. Reson. 48*, 286−298.
Stombaugh, N. A., Sundquist, J. E., Burris, S. H., & Orme-Johnson, W. H. (1976) *Biochemistry 15*, 2633−2641.
Wishart, D. S., Sykes, B. D., & Richards, F. M. (1991) *J. Mol. Biol. 222*, 311−333.
Wüthrich, K., (1986) *NMR of Proteins and Nucleic Acids*, John Wiley & Sons, New York, NY.